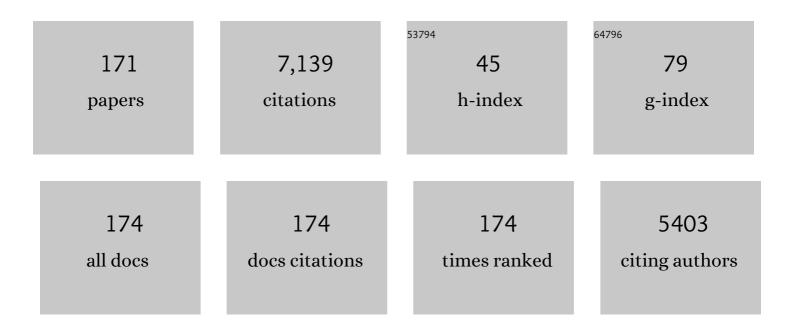
List of Publications by Year in descending order

Source: https://exaly.com/author-pdf/920958/publications.pdf Version: 2024-02-01



#	Article	IF	CITATIONS
1	Polymorphous Crystallization and Multiple Melting Behavior of Poly(<scp>l</scp> -lactide): Molecular Weight Dependence. Macromolecules, 2007, 40, 6898-6905.	4.8	591
2	Polymorphism and isomorphism in biodegradable polyesters. Progress in Polymer Science, 2009, 34, 605-640.	24.7	527
3	Polymorphic Transition in Disordered Poly(<scp>l</scp> -lactide) Crystals Induced by Annealing at Elevated Temperatures. Macromolecules, 2008, 41, 4296-4304.	4.8	305
4	Enthalpy Relaxation and Embrittlement of Poly(<scp>l</scp> -lactide) during Physical Aging. Macromolecules, 2007, 40, 9664-9671.	4.8	222
5	Temperature-Variable FTIR and Solid-State ¹³ C NMR Investigations on Crystalline Structure and Molecular Dynamics of Polymorphic Poly(<scp> </scp> -lactide) and Poly(<scp> </scp> -lactide)/Poly(<scp>d</scp> -lactide) Stereocomplex. Macromolecules, 2012, 45, 189-197.	4.8	206
6	Effect of crystallization temperature on crystal modifications and crystallization kinetics of poly(<scp>L</scp> ″actide). Journal of Applied Polymer Science, 2008, 107, 54-62.	2.6	204
7	Layered Metal Phosphonate Reinforced Poly(<scp>l</scp> -lactide) Composites with a Highly Enhanced Crystallization Rate. ACS Applied Materials & amp; Interfaces, 2009, 1, 402-411.	8.0	187
8	Competitive Stereocomplexation, Homocrystallization, and Polymorphic Crystalline Transition in Poly(<scp>l</scp> -lactic acid)/Poly(<scp>d</scp> -lactic acid) Racemic Blends: Molecular Weight Effects. Journal of Physical Chemistry B, 2015, 119, 6462-6470.	2.6	172
9	Blending Effects on Polymorphic Crystallization of Poly(<scp>l</scp> -lactide). Macromolecules, 2009, 42, 3374-3380.	4.8	142
10	Stereocomplex crystallization of high-molecular-weight poly(l-lactic acid)/poly(d-lactic acid) racemic blends promoted by a selective nucleator. Polymer, 2015, 63, 144-153.	3.8	117
11	Core–Shell Structure, Biodegradation, and Drug Release Behavior of Poly(lactic acid)/Poly(ethylene) Tj ETQq1 1 1527-1536.	0.784314 3.5	rgBT /Overl 112
12	Crystallization of biodegradable and biobased polyesters: Polymorphism, cocrystallization, and structure-property relationship. Progress in Polymer Science, 2020, 109, 101291.	24.7	111
13	Polymorphic Crystalline Structure and Crystal Morphology of Enantiomeric Poly(lactic acid) Blends Tailored by a Self-Assemblable Aryl Amide Nucleator. ACS Sustainable Chemistry and Engineering, 2016, 4, 2680-2688.	6.7	110
14	Crystallization behavior and mechanical properties of bio-based green composites based on poly(L-lactide) and kenaf fiber. Journal of Applied Polymer Science, 2007, 105, 1511-1520.	2.6	109
15	Roles of Physical Aging on Crystallization Kinetics and Induction Period of Poly(<scp> </scp> -lactide). Macromolecules, 2008, 41, 8011-8019.	4.8	105
16	Polymorphic Crystallization and Phase Transition of Poly(butylene adipate) in Its Miscible Crystalline/Crystalline Blend with Poly(vinylidene fluoride). Macromolecules, 2010, 43, 8610-8618.	4.8	95
17	Fractionated crystallization, polymorphic crystalline structure, and spherulite morphology of poly(butylene adipate) in its miscible blend with poly(butylene succinate). Polymer, 2011, 52, 3460-3468.	3.8	83
18	Exclusive Stereocomplex Crystallization of Linear and Multiarm Star-Shaped High-Molecular-Weight Stereo Diblock Poly(lactic acid)s. Journal of Physical Chemistry B, 2015, 119, 14270-14279.	2.6	83

#	Article	IF	CITATIONS
19	Stereocomplexation of high-molecular-weight enantiomeric poly(lactic acid)s enhanced by miscible polymer blending with hydrogen bond interactions. Polymer, 2016, 98, 80-87.	3.8	80
20	Mechanical and thermal properties of poly(butylene succinate)/plant fiber biodegradable composite. Journal of Applied Polymer Science, 2010, 115, 3559-3567.	2.6	79
21	Programmable Reversible Shape Transformation of Hydrogels Based on Transient Structural Anisotropy. Advanced Materials, 2020, 32, e2001693.	21.0	77
22	Uracil as Nucleating Agent for Bacterial Poly[(3â€Hydroxybutyrate)â€ <i>co</i> â€(3â€hydroxyhexanoate)] Copolymers. Macromolecular Bioscience, 2009, 9, 585-595.	4.1	75
23	Dualâ€Crosslink Physical Hydrogels with High Toughness Based on Synergistic Hydrogen Bonding and Hydrophobic Interactions. Macromolecular Rapid Communications, 2018, 39, e1700806.	3.9	72
24	A Facile Approach To Prepare Tough and Responsive Ultrathin Physical Hydrogel Films as Artificial Muscles. ACS Applied Materials & Interfaces, 2017, 9, 34349-34355.	8.0	70
25	Hydrophobic association mediated physical hydrogels with high strength and healing ability. Polymer, 2016, 100, 60-68.	3.8	68
26	ABA-Type Thermoplastic Elastomers Composed of Poly(ε-caprolactone- <i>co</i> -δ-valerolactone) Soft Midblock and Polymorphic Poly(lactic acid) Hard End blocks. ACS Sustainable Chemistry and Engineering, 2016, 4, 121-128.	6.7	65
27	Alternating poly(lactic acid)/poly(ethylene-co-butylene) supramolecular multiblock copolymers with tunable shape memory and self-healing properties. Polymer Chemistry, 2015, 6, 5899-5910.	3.9	64
28	Conformational and microstructural characteristics of poly(L-lactide) during glass transition and physical aging. Journal of Chemical Physics, 2008, 129, 184902.	3.0	63
29	Synergetic Chemical and Physical Programming for Reversible Shape Memory Effect in a Dynamic Covalent Network with Two Crystalline Phases. ACS Macro Letters, 2019, 8, 682-686.	4.8	62
30	Enhanced Nucleation and Crystallization of Poly(<scp>l</scp> -lactic acid) by Immiscible Blending with Poly(vinylidene fluoride). Industrial & Engineering Chemistry Research, 2014, 53, 3148-3156.	3.7	60
31	Interactions between an Anticancer Drug and Polymeric Micelles Based on Biodegradable Polyesters. Macromolecular Bioscience, 2008, 8, 1116-1125.	4.1	56
32	Nucleation Effects of Nucleobases on the Crystallization Kinetics of Poly(<scp>L</scp> â€lactide). Macromolecular Materials and Engineering, 2012, 297, 670-679.	3.6	55
33	In Situ Formation and Gelation Mechanism of Thermoresponsive Stereocomplexed Hydrogels upon Mixing Diblock and Triblock Poly(Lactic Acid)/Poly(Ethylene Glycol) Copolymers. Journal of Physical Chemistry B, 2015, 119, 6471-6480.	2.6	55
34	Light oded Digital Crystallinity Patterns Toward Bioinspired 4D Transformation of Shapeâ€Memory Polymers. Advanced Functional Materials, 2020, 30, 2000522.	14.9	55
35	Promoted Stereocomplex Crystallization in Supramolecular Stereoblock Copolymers of Enantiomeric Poly(Lactic Acid)s. Crystal Growth and Design, 2016, 16, 1502-1511.	3.0	54
36	Temperature and pH-dependent swelling and copper(<scp>ii</scp>) adsorption of poly(N-isopropylacrylamide) copolymer hydrogel. RSC Advances, 2015, 5, 62091-62100.	3.6	52

#	Article	IF	CITATIONS
37	Click chemistry synthesis, stereocomplex formation, and enhanced thermal properties of well-defined poly(<scp>l</scp> -lactic acid)-b-poly(<scp>d</scp> -lactic acid) stereo diblock copolymers. Polymer Chemistry, 2017, 8, 1006-1016.	3.9	52
38	Thermoresponsive physical hydrogels of poly(lactic acid)/poly(ethylene glycol) stereoblock copolymers tuned by stereostructure and hydrophobic block sequence. Soft Matter, 2016, 12, 4628-4637.	2.7	51
39	Crystallization behavior and crystalline structural changes of poly(glycolic acid) investigated via temperature-variable WAXD and FTIR analysis. CrystEngComm, 2016, 18, 7894-7902.	2.6	50
40	Enhancement of Crystallizability and Control of Mechanical and Shape-Memory Properties for Amorphous Enantiopure Supramolecular Copolymers via Stereocomplexation. Macromolecules, 2015, 48, 7872-7881.	4.8	49
41	Preferential Formation of β-Form Crystals and Temperature-Dependent Polymorphic Structure in Supramolecular Poly(<scp> </scp> -lactic acid) Bonded by Multiple Hydrogen Bonds. Macromolecules, 2017, 50, 8619-8630.	4.8	49
42	Isomorphic Crystallization of Poly(hexamethylene adipate- <i>co</i> -butylene adipate): Regulating Crystal Modification of Polymorphic Polyester from Internal Crystalline Lattice. Macromolecules, 2010, 43, 6429-6437.	4.8	48
43	Effects of Crystallization Temperature of Poly(vinylidene fluoride) on Crystal Modification and Phase Transition of Poly(butylene adipate) in Their Blends: A Novel Approach for Polymorphic Control. Journal of Physical Chemistry B, 2012, 116, 1265-1272.	2.6	48
44	Effects of Hostâ^'Guest Stoichiometry of α-Cyclodextrinâ^'Aliphatic Polyester Inclusion Complexes and Molecular Weight of Guest Polymer on the Crystallization Behavior of Aliphatic Polyesters. Macromolecules, 2007, 40, 7244-7251.	4.8	47
45	Competing Stereocomplexation and Homocrystallization of Poly(<scp>l</scp> -lactic) Tj ETQq1 1 0.784314 rgB Polymers. Journal of Physical Chemistry B, 2017, 121, 6934-6943.	7 /Overlock 2.6	2 10 Tf 50 42 46
46	Enantiomeric blends of high-molecular-weight poly(lactic acid)/poly(ethylene glycol) triblock copolymers: Enhanced stereocomplexation and thermomechanical properties. Polymer, 2016, 103, 376-386.	3.8	45
47	Crystallization kinetics and crystalline structure of biodegradable Poly(ethylene adipate). Polymer, 2010, 51, 807-815.	3.8	44
48	Crystalline and Spherulitic Morphology of Polymers Crystallized in Confined Systems. Crystals, 2017, 7, 147.	2.2	44
49	Role of Chain Entanglements in the Stereocomplex Crystallization between Poly(lactic acid) Enantiomers. ACS Macro Letters, 2021, 10, 1023-1028.	4.8	44
50	Poly(<scp>L</scp> â€lactide)/layered double hydroxides nanocomposites: Preparation and crystallization behavior. Journal of Polymer Science, Part B: Polymer Physics, 2008, 46, 2222-2233.	2.1	43
51	Fractional Crystallization Kinetics and Formation of Metastable β-Form Homocrystals in Poly(<scp>l</scp> -lactic acid)/Poly(<scp>d</scp> -lactic acid) Racemic Blends Induced by Precedingly Formed Stereocomplexes. Macromolecules, 2019, 52, 4655-4665.	4.8	43
52	DNA-functionalized thermoresponsive bioconjugates synthesized via ATRP and click chemistry. Polymer, 2011, 52, 895-900.	3.8	42
53	Isomorphic crystallization of aliphatic copolyesters derived from 1,6-hexanediol: Effect of the chemical structure of comonomer units on the extent of cocrystallization. Polymer, 2011, 52, 2667-2676.	3.8	41
54	Preferential Stereocomplex Crystallization in Enantiomeric Blends of Cellulose Acetate- <i>g</i> -Poly(lactic acid)s with Comblike Topology. Journal of Physical Chemistry B, 2015, 119, 12689-12698.	2.6	41

#	Article	IF	CITATIONS
55	Crystalline Phase of Isomorphic Poly(hexamethylene sebacate- <i>co</i> -hexamethylene adipate) Copolyester: Effects of Comonomer Composition and Crystallization Temperature. Macromolecules, 2010, 43, 2925-2932.	4.8	40
56	Bioinspired Dualâ€Mode Temporal Communication via Digitally Programmable Phaseâ€Change Materials. Advanced Materials, 2021, 33, e2008119.	21.0	40
57	A strong and tough interpenetrating network hydrogel with ultrahigh compression resistance. Soft Matter, 2014, 10, 3850.	2.7	39
58	Synthesis of end-functionalized hydrogen-bonding poly(lactic acid)s and preferential stereocomplex crystallization of their enantiomeric blends. Polymer Chemistry, 2016, 7, 4891-4900.	3.9	39
59	Effect of orotic acid as a nucleating agent on the crystallization of bacterial poly(3â€hydroxybutyrateâ€ <i>co</i> â€3â€hydroxyhexanoate) copolymers. Journal of Applied Polymer Science, 2009, 114, 1287-1294.	2.6	38
60	Temperatureâ€dependent polymorphic crystalline structure and melting behavior of poly(butylene) Tj ETQq0 0 0 Physics, 2009, 47, 1997-2007.	rgBT /Ove 2.1	erlock 10 Tf 5 38
61	Nucleation mechanism of polyhydroxybutyrate and poly(hydroxybutyrateâ€ <i>co</i> â€hydroxyhexanoate) crystallized by orotic acid as a nucleating agent. Journal of Applied Polymer Science, 2010, 115, 709-715.	2.6	36
62	Thermoresponsive Micellization and Micellar Stability of Poly(<i>N</i> -isopropylacrylamide)- <i>b</i> -DNA Diblock and Miktoarm Star Polymers. Langmuir, 2012, 28, 14347-14356.	3.5	36
63	Heating and Annealing Induced Structural Reorganization and Embrittlement of Solution-Crystallized Poly(<scp>l</scp> -lactic acid). Macromolecules, 2014, 47, 8126-8130.	4.8	36
64	Stereocomplexed and Homochiral Polyurethane Elastomers with Tunable Crystallizability and Multishape Memory Effects. ACS Macro Letters, 2018, 7, 233-238.	4.8	36
65	Selective adsorption and high recovery of La3+ using graphene oxide/poly (N-isopropyl) Tj ETQq1 1 0.784314 rgE	3T /Overlo 12.7	ck 10 Tf 50 3
66	Structure and Morphology of Poly(lactic acid) Stereocomplex Nanofiber Shish Kebabs. ACS Macro Letters, 2020, 9, 103-107.	4.8	33
67	Crystallization kinetics of bacterial poly(3â€hydroxylbutyrate) copolyesters with cyanuric acid as a nucleating agent. Journal of Applied Polymer Science, 2013, 129, 1374-1382.	2.6	31
68	Stress-Free Two-Way Shape Memory Effects of Semicrystalline Polymer Networks Enhanced by Self-Nucleated Crystallization. ACS Macro Letters, 2020, 9, 1325-1331.	4.8	31
69	Kenaf fiber/poly(εâ€caprolactone) biocomposite with enhanced crystallization rate and mechanical properties. Journal of Applied Polymer Science, 2008, 107, 3512-3519.	2.6	30
70	Nucleation Effect of Layered Metal Phosphonate on Crystallization of Bacterial Poly[(3â€hydroxybutyrate)â€ <i>co</i> â€(3â€hydroxyhexanoate)]. Macromolecular Materials and Engineering, 2011, 296, 103-112.	3.6	30
71	Synthesis and Crystallization of Poly(vinyl acetate)- <i>g</i> Poly(<scp>l</scp> -lactide) Graft Copolymer with Controllable Graft Density. Industrial & Engineering Chemistry Research, 2013, 52, 12897-12905.	3.7	30
72	Polylactide-b-poly(ethylene-co-butylene)-b-polylactide thermoplastic elastomers: role of polylactide crystallization and stereocomplexation on microphase separation, mechanical and shape memory properties. RSC Advances, 2014, 4, 47965-47976.	3.6	30

#	Article	IF	CITATIONS
73	Monodomain hydrogels prepared by shear-induced orientation and subsequent gelation. RSC Advances, 2016, 6, 95239-95245.	3.6	30
74	Stretch-Induced \hat{l}_{\pm} -to- \hat{l}^2 Crystal Transition and Lamellae Structural Evolution of Poly(butylene) Tj ETQq0 0 0 rgBT /	Oyerlock	10 Jf 50 702
75	Double network hydrogels with highly enhanced toughness based on a modified first network. Soft Matter, 2017, 13, 4148-4158.	2.7	26
76	High strength of hybrid double-network hydrogels imparted by inter-network ionic bonds. Journal of Materials Chemistry B, 2019, 7, 324-333.	5.8	26
77	Stretch-induced crystalline structural evolution and cavitation of poly(butylene adipate-ran-butylene) Tj ETQq1 1	0. <u>78</u> 4314	rgBT /Overlo
78	Differential diffusion driven far-from-equilibrium shape-shifting of hydrogels. Nature Communications, 2021, 12, 6155.	12.8	26
79	Stereocomplexed physical hydrogels with high strength and tunable crystallizability. Soft Matter,	2.7	24

Fractional Crystallization and Phase Segregation in Binary Miscible Poly(butylene) Tj ETQq0 0 0 rgBT /Overlock 10 Tf 50 467 Td (succina 80
Macromolecular Materials and Engineering, 2013, 298, 201-209.

81			23
82	Crystallization-Driven Formation of Diversified Assemblies for Supramolecular Poly(lactic acid)s in Solution. Crystal Growth and Design, 2017, 17, 2498-2506.	3.0	23
83	Tammann Analysis of the Molecular Weight Selection of Polymorphic Crystal Nucleation in Symmetric	4.8	23

84	Triple Stimuli-Responsive <i>N</i> -Isopropylacrylamide Copolymer toward Metal Ion Recognition and Adsorption via a Thermally Induced Sol–Gel Transition. Industrial & Engineering Chemistry Research, 2017, 56, 1223-1232.	3.7	22
85	Poly(lactic acid)/poly(ethylene glycol) stereocomplexed physical hydrogels showing thermally-induced gel–sol–gel multiple phase transitions. Materials Chemistry Frontiers, 2018, 2, 313-322.	5.9	21
86	Polyhedral Oligomeric Silsesquioxane―and Fullereneâ€Endâ€Capped Poly(<i>ε</i> â€caprolactone). Macromolecular Chemistry and Physics, 2008, 209, 1191-1197.	2.2	19
87	Poly(lactic acid)/poly(ethylene glycol) supramolecular diblock copolymers based on three-fold complementary hydrogen bonds: Synthesis, micellization, and stimuli responsivity. Polymer, 2016, 90, 122-131.	3.8	19
88	Fast photothermal poly(NIPAM- <i>co</i> -β-cyclodextrin) supramolecular hydrogel with self-healing through host–guest interaction for intelligent light-controlled switches. Soft Matter, 2020, 16, 10558-10566.	2.7	19
89	Fullerene Endâ€Capped Biodegradable Poly(<i>ε</i> â€caprolactone). Macromolecular Chemistry and Physics, 2008, 209, 104-111.	2.2	18

Polymorphic homocrystallization and phase behavior of high-molecular-weight Poly(L-lactic) Tj ETQq0 0 0 rgBT /Overlock 10 Tf 50 67 Td 3.8 18 miscible blending. Polymer, 2020, 201, 122597.

#	Article	IF	CITATIONS
91	Effects of Complementary DNA and Salt on the Thermoresponsiveness of Poly(<i>N</i> -isopropylacrylamide)- <i>b</i> -DNA. Langmuir, 2016, 32, 1148-1154.	3.5	17
92	Sequence-Rearranged Cocrystalline Polymer Network with Shape Reconfigurability and Tunable Switching Temperature. ACS Macro Letters, 2020, 9, 588-594.	4.8	17
93	Solventâ€free ringâ€opening polymerization of lactones with hydrogenâ€bonding bisurea catalyst. Journal of Polymer Science Part A, 2019, 57, 90-100.	2.3	16
94	Structural characterization of nanoparticles from thermoresponsive poly(N-isopropylacrylamide)-DNA conjugate. Journal of Colloid and Interface Science, 2012, 374, 315-320.	9.4	15
95	Highly enhanced toughness of interpenetrating network hydrogel by incorporating poly(ethylene) Tj ETQq1 1 C).784314 rg	gBT_/Overlock
96	Thermoresponsive poly(<i>ϵ</i> -caprolactone)- <i>graft</i> -poly(<i>N</i> -isopropylacrylamide) graft copolymers prepared by a combination of ring-opening polymerization and sequential azide-alkyne click chemistry. Polymer International, 2015, 64, 389-396.	3.1	15
97	Solution and aqueous miniemulsion polymerization of vinyl chloride mediated by a fluorinated xanthate. Journal of Polymer Science Part A, 2016, 54, 2092-2101.	2.3	15
98	Temperature-dependent crystalline structure and phase transition of poly(butylene adipate) end-functionalized by multiple hydrogen-bonding groups. Physical Chemistry Chemical Physics, 2018, 20, 26479-26488.	2.8	15
99	Formation of Mesomorphic Polymorph, Thermal-Induced Phase Transition, and Crystalline Structure-Dependent Degradable and Mechanical Properties of Poly(<i>p</i> -dioxanone). Crystal Growth and Design, 2019, 19, 166-176.	3.0	15
100	Bioinspired Stimuliâ€Responsive Hydrogel with Reversible Switching and Fluorescence Behavior Served as Light ontrolled Soft Actuators. Macromolecular Materials and Engineering, 2021, 306, 2100379.	3.6	15
101	Crystallization behavior and mechanical properties of poly(εâ€caprolactone)/cyclodextrin biodegradable composites. Journal of Applied Polymer Science, 2009, 112, 2351-2357.	2.6	14
102	Synthesis, micellization, and thermally-induced macroscopic micelle aggregation of poly(vinyl) Tj ETQq0 0 0 rgE	3T /Qverloc	k 10 Tf 50 30 14
103	Stereocomplexed and homocrystalline thermo-responsive physical hydrogels with a tunable network structure and thermo-responsiveness. Journal of Materials Chemistry B, 2020, 8, 7947-7955.	5.8	14
104	Thermoresponsivity, Micelle Structure, and Thermal-Induced Structural Transition of an Amphiphilic Block Copolymer Tuned by Terminal Multiple H-Bonding Units. Langmuir, 2020, 36, 956-965.	3.5	14
105	Tuning the Thermoresponsivity of Amphiphilic Copolymers via Stereocomplex Crystallization of Hydrophobic Blocks. ACS Macro Letters, 2019, 8, 357-362.	4.8	13
106	Homocrystalline mesophase formation and multistage structural transitions in stereocomplexable racemic blends of block copolymers. Polymer, 2020, 189, 122180.	3.8	13
107	Separate crystallization and melting of polymer blocks and hydrogen bonding units in double-crystalline supramolecular polymers. Polymer, 2021, 222, 123670.	3.8	13
108	Influence of Ce/Nb Molar Ratios on Oxygen-Rich CexNb1-xO4+δ Materials for Catalytic Combustion of VOCs in the Process of Polyether Polyol Synthesis. Catalysis Letters, 2022, 152, 523-537.	2.6	13

	Р	ΈN	۱GJ	U	P	٨N
--	---	----	-----	---	---	----

#	Article	IF	CITATIONS
109	Critical role of the conformation of comonomer units in isomorphic crystallization of poly(hexamethylene adipate-co-butylene adipate) forming Poly(hexamethylene adipate) type crystal. Polymer, 2011, 52, 5204-5211.	3.8	12
110	Fractionated crystallization and selfâ€nucleation behavior of poly(ethylene oxide) in its miscible blends with poly(3â€hydroxybutyrate). Journal of Applied Polymer Science, 2010, 117, 3013-3022.	2.6	11
111	Reactive blend of epoxyâ€novolac resin and epoxideâ€ŧerminated lowâ€molecularâ€weight poly(phenylene) Tj ET(Qq1 1 0.7 2.6	84314 rg8 11
112	Stereocomplex Crystallization of Polymers With Complementary Configurations. , 2018, , 535-573.		11
113	Roles of Conformational Flexibility in the Crystallization of Stereoirregular Polymers. Macromolecules, 2021, 54, 5705-5718.	4.8	11
114	Retarded Crystallization and Promoted Phase Transition of Freeze-Dried Polybutene-1: Direct Evidence for the Critical Role of Chain Entanglement. ACS Macro Letters, 2022, 11, 257-263.	4.8	11
115	Isodimorphic Crystallization and Tunable γ–α Phase Transition in Aliphatic Copolyamides: Critical Roles of Comonomer Defects and Conformational Evolution. Macromolecules, 2022, 55, 6090-6101.	4.8	11
116	Polymorphic Packing and Dynamics of Biodegradable Poly(3-hydroxypropionate). Journal of Physical Chemistry B, 2008, 112, 9684-9692.	2.6	10
117	Fractional Crystallization Kinetics of Poly(ethylene oxide) in Its Blends with Poly(butylene succinate): Molecular Weight Effects. Macromolecular Materials and Engineering, 2013, 298, 919-927.	3.6	10
118	Kinetic Insights into Marangoni Effect-Assisted Preparation of Ultrathin Hydrogel Films. Langmuir, 2018, 34, 12310-12317.	3.5	10
119	Polymorphic Crystal Transition and Lamellae Structural Evolution of Poly(<i>p</i> -dioxanone) Induced by Annealing and Stretching. Journal of Physical Chemistry B, 2019, 123, 3822-3831.	2.6	10
120	Gelatin/Poly(ethylene oxide) Blend Films with Compositional Gradient: Fabrication and Characterization. Macromolecular Materials and Engineering, 2010, 295, 256-262.	3.6	9
121	A facile self-templating synthesis of carbon frameworks with tailored hierarchical porosity for enhanced energy storage performance. Chemical Communications, 2017, 53, 5028-5031.	4.1	9
122	Morphology and blowing agent encapsulation efficiency of vinylidene chloride copolymer microspheres synthesized by suspension polymerization in the presence of a blowing agent. Journal of Applied Polymer Science, 2017, 134, .	2.6	9
123	Stepwise Crystallization and Induced Microphase Separation in Nucleobase-Monofunctionalized Supramolecular Poly(ε-caprolactone). Macromolecules, 2021, 54, 846-857.	4.8	9
124	Multistage Structural Ordering and Crystallization of Poly(trimethylene terephthalate) during Sub- <i>T</i> _g Stretching: Synergetic Effects of Chain Orientation and Conformational Transition. Macromolecules, 2022, 55, 252-261.	4.8	9
125	Poly(εâ€caprolactone)â€ <i>graft</i> â€poly(<i>N</i> â€isopropylacrylamide) amphiphilic copolymers prepared by a combination of ringâ€opening polymerization and atom transfer radical polymerization: Synthesis, selfâ€assembly, and thermoresponsive property. Journal of Applied Polymer Science, 2014, 131, .	2.6	8
126	Controlled coâ€delivery of hydrophilic and hydrophobic drugs from thermosensitive and crystallizable copolymer nanoparticles. Journal of Applied Polymer Science, 2016, 133, .	2.6	8

#	Article	IF	CITATIONS
127	Nucleobase-monofunctionalized supramolecular poly(<scp>l</scp> -lactide): controlled synthesis, competitive crystallization, and structural organization. Polymer Chemistry, 2021, 12, 3461-3470.	3.9	8
128	Synthesis and characterization of fullerene grafted poly(ε aprolactone). Journal of Applied Polymer Science, 2008, 107, 4029-4035.	2.6	7
129	Miscibility and Physical Properties of Poly(3â€hydroxybutyrate <i>â€coâ€</i> 3â€hydroxyhexanoate)/Poly(ethylene oxide) Binary Blends. Macromolecular Materials and Engineering, 2009, 294, 868-876.	3.6	7
130	Aqueous RAFT polymerization of acrylamide: A convenient method for polyacrylamide with narrow molecular weight distribution. Chinese Journal of Polymer Science (English Edition), 2017, 35, 123-129.	3.8	7
131	Temperature-dependent Crystallization and Phase Transition of Poly(L-lactic acid)/CO2 Complex Crystals. Chinese Journal of Polymer Science (English Edition), 2021, 39, 484-492.	3.8	7
132	Crystallizationâ€driven selfâ€assembly of semicrystalline block copolymers and endâ€functionalized polymers: A minireview. Journal of Polymer Science, 2022, 60, 2136-2152.	3.8	7
133	Evolution of thermal behavior, mechanical properties, and microstructure in stereocomplexable poly(lactic acid) during physical ageing. Polymer, 2022, 249, 124840.	3.8	7
134	Preparation of hierarchical porous carbons from amphiphilic poly(vinylidene chloride-co-methyl) Tj ETQq0 0 0 rgBT Microporous and Mesoporous Materials, 2014, 196, 199-207.	/Overlock 4.4	2 10 Tf 50 46 6
135	Kinetic and Molecular Weight Modeling of Miniemulsion Polymerization Initiated by Oilâ€Soluble Initiators. Macromolecular Chemistry and Physics, 2015, 216, 884-893.	2.2	6
136	Synthesis of random and block copolymers of vinyl chloride and vinyl acetate by <scp>RAFT</scp> miniemulsion polymerizations mediated by a fluorinated xanthate. Journal of Applied Polymer Science, 2017, 134, 45074.	2.6	6
137	Promoted stereocomplex formation and twoâ€step crystallization kinetics of poly(<scp>l</scp> ″actic) Tj ETQq e10057.	1 1 0.784 0.8	314 rgBT /C 6
138	Self-evolving materials based on metastable-to-stable crystal transition of a polymorphic polyolefin. Materials Horizons, 2022, 9, 756-763.	12.2	6
139	Glassy Alfa-Relaxation Promotes Surprising Homo-Crystal Nucleation in the Low-Molar-Mass Enantiomeric Poly(lactic acid) Blend. Macromolecules, 2022, 55, 4614-4623.	4.8	6
140	Polymorphic crystallization of poly(butylene adipate) and its copolymer: Effect of poly(vinyl alcohol). Journal of Applied Polymer Science, 2014, 131, .	2.6	5
141	Modeling for primary radical desorption in miniemulsion polymerization initiated by oilâ€soluble initiator. AICHE Journal, 2014, 60, 3276-3285.	3.6	5
142	Stabilizer-Free Aqueous Two-Phase Copolymerization of Acrylamide and Cationic Monomer: Role of Electrostatic Interactions in the Phase Separation, Colloid Morphology, and Stability. Industrial & Engineering Chemistry Research, 2014, 53, 14664-14672.	3.7	5
143	Amphiphilic quasi-block copolymers and their self-assembled nanoparticles via thermally induced interfacial absorption in miniemulsion polymerization. RSC Advances, 2015, 5, 50118-50125.	3.6	5
144	Nanostructured poly(<scp> </scp> -lactic acid)–poly(ethylene glycol)–poly(<scp> </scp> -lactic acid) triblock copolymers and their CO ₂ /O ₂ permselectivity. RSC Advances, 2019, 9, 12354-12364.	3.6	5

#	Article	IF	CITATIONS
145	Controllable crystallization and lamellar organization in nucleobase-functionalized supramolecular poly(lactic acid)s: Role of poly(lactic acid) stereostructure. Polymer, 2021, 232, 124148.	3.8	5
146	Nitroxide-mediated polymerization of methyl methacrylate by 4,4′-dimethoxydiphenyl-based alkoxyamine. RSC Advances, 2016, 6, 73842-73847.	3.6	4
147	Rate acceleration for 4,4′-dimethoxydiphenyl nitroxide mediated polymerization of methyl methacrylate. RSC Advances, 2016, 6, 97995-98000.	3.6	4
148	Role of salt in the aqueous two-phase copolymerization of acrylamide and cationic monomers: from screening to anion-bridging. RSC Advances, 2016, 6, 59352-59359.	3.6	4
149	Controllable Poly(L-lactic acid) Soft Film with Respirability and Its Effect on Strawberry Preservation. Polymer Science - Series A, 2021, 63, 77-90.	1.0	4
150	Temperature-dependent crystal structure and structural evolution of poly(glycolide-co-lactide) induced by comonomeric defect inclusion/exclusion. Polymer, 2021, 227, 123867.	3.8	4
151	Anisotropic bilayer hydrogels with synergistic photochromism behaviors for light-controlled actuators. Journal of Materials Science, 2021, 56, 16324-16338.	3.7	4
152	Fractionated Crystallization Kinetics and Polymorphic Homocrystalline Structure of Poly(L-lactic) Tj ETQq0 0 0 rgE	3T /Overloo 3.8	ck 10 Tf 50 4 4
153	Structural Evolutions of Initially Amorphous Polymers during Nearâ€ <i>T</i> _g Stretching: A Minireview of Recent Progresses. Macromolecular Chemistry and Physics, 2022, 223, .	2.2	4
154	One-step preparation of hierarchical porous carbons from poly(vinylidene chloride)-based block copolymers. Journal of Materials Science, 2014, 49, 1090-1098.	3.7	3
155	Effect of hydration layer on the structure of thermoâ€sensitive nanocapsules. Journal of Applied Polymer Science, 2014, 131, .	2.6	3
156	<i>Ab initio</i> emulsion RAFT polymerization of vinylidene chloride mediated by amphiphilic macroâ€RAFT agents. Journal of Applied Polymer Science, 2014, 131, .	2.6	3
157	Free volume characteristics of 2, 2â€bistrifluoromethyl â€4,5â€difluoroâ€1,3â€dioxole―co â€ŧetrafluoroethyler copolymers: Effect of composition and molecular weight. Journal of Polymer Science, 2021, 59, 754-763.	1e 3.8	3
158	Microstructurally tunable pickering emulsions stabilized by poly(ethylene) Tj ETQq0 0 0 rgBT /Overlock 10 Tf 50 2 architecture. Food Chemistry, 2022, 374, 131827.	27 Td (gly 8.2	vcol)-b-poly(Î 3
159	Photothermal driven polymorph pattern in semicrystalline polymers towards programmable shape morphing. Chemical Engineering Journal, 2022, 446, 137346.	12.7	3
160	Unique multiple soluble–insoluble phase transitions in aqueous two-phase copolymerization of acrylamide and a weakly charged comonomer. Soft Matter, 2014, 10, 8913-8922.	2.7	2
161	Role of added amphiphilic cationic polymer in the stabilization of inverse emulsions. Colloid and Polymer Science, 2017, 295, 2207-2215.	2.1	2
162	Hierarchical ordering and multilayer structure of poly(ε-caprolactone) end-functionalized by a liquid crystalline unit: role of polymer crystallization. Polymer Chemistry, 2021, 12, 4175-4183.	3.9	2

#	Article	IF	CITATIONS
163	Polymorphic Phase Formation of Liquid Crystals Distributed in Semicrystalline Polymers: An Indicator of Interlamellar and Interspherulitic Segregation. Journal of Physical Chemistry Letters, 2021, 12, 4378-4384.	4.6	2
164	Controllable formation of unusual homocrystals in poly(<scp>L</scp> -lactic) Tj ETQq0 0 0 rgBT /Overlock 10 Tf 50 pre-existing stereocomplexes. Journal of Applied Crystallography, 2020, 53, 1266-1275.	707 Td (a 4.5	icid)/poly(< 2
165	Asymmetric Molecular Dynamics and Anisotropic Phase Separation in the Cocrystal of the Crystalline/Crystalline Polymer Blend. ACS Macro Letters, 2022, 11, 193-198.	4.8	2
166	Light-Induced Crystalline Size Heterogeneity of Polymers Enables Programmable Writing, Morphing, and Mechanical Performance Designing. ACS Macro Letters, 2022, 11, 739-746.	4.8	2
167	Online monitoring of drop/particle size and size distribution in liquid–liquid dispersions and suspension polymerizations by optical reflectance measurements. Journal of Applied Polymer Science, 2016, 133, .	2.6	1
168	CURING KINETIC MODEL OF THE 2-ETHYL-4-METHYLIMIDAZOLE/EPOXY SYSTEM. Acta Polymerica Sinica, 2006, 006, 21-25.	0.0	1
169	Unusual Soluble–Insoluble–Soluble Phase Transition in Two-Phase Copolymerization of Acrylamide and an Anionic Comonomer in a Poly(ethylene glycol) Aqueous Solution. Industrial & Engineering Chemistry Research, 2014, 53, 10681-10687.	3.7	0
170	Polymorphic crystalline structure and diversified crystalline morphology of poly(butylene adipate) blended with lowâ€molecularâ€mass liquid crystals. Polymer Crystallization, 2020, 3, e10099.	0.8	0
171	2,2â€Bistrifluoromethylâ€4,5â€difluoroâ€1,3â€dioxole― <i>co</i> â€ŧetrafluoroethylene copolymers with differe compositions: Synthesis, chain and condensed matter structures and optical properties. Journal of Applied Polymer Science, 0, , .	nt 2.6	0